Int J Adv Manuf Technol (2014) 73:1095–1104
DOI 10.1007/s00170-014-5910-8

ORIGINAL ARTICLE

Robust H_∞ sliding mode control with pole placement for a fluid power electrohydraulic actuator (EHA) system

Hui Zhang · Xiaotao Liu · Junmin Wang · Hamid Reza Karimi

Received: 25 January 2014 / Accepted: 29 April 2014 / Published online: 13 May 2014

Abstract In this paper, we exploit the sliding mode control problem for a fluid power electrohydraulic actuator (EHA) system. To characterize the nonlinearity of the friction, the EHA system is modeled as a linear system with a system uncertainty. Practically, it is assumed that the system is also subject to the load disturbance and the external noise. An integral sliding mode controller is proposed to design. The advanced techniques such as the H_∞ control and the regional pole placement are employed to derive the optimal feedback gain which can be calculated by solving a necessary and sufficient condition in the form of linear matrix inequality. A sliding mode control law is developed such that the sliding mode reaching law is satisfied. Simulation and comparison results show the effectiveness of the proposed design method.

Keywords Sliding mode control · H_∞ control · Pole placement · Linear matrix inequalities (LMIs)

H. Zhang (✉)
Merchant Marine College, Shanghai Maritime University,
1550 Haigang Avenue, 201306 Shanghai, China
e-mail: huizhang285@gmail.com

X. Liu
Department of Mechanical Engineering, University of Victoria,
PO Box 3055, STN CSC, Victoria, BC V8W 3P6, Canada

J. Wang
Department of Mechanical and Aerospace Engineering,
The Ohio State University, Columbus, OH 43210, USA
e-mail: wang.1381@osu.edu

H. R. Karimi
Faculty of Engineering and Science, University of Agder, Grimstad,
Norway
e-mail: hamid.r.karimi@uia.no

1 Introduction

The subject in this paper is a fluid power electrohydraulic actuator (EHA) system which is controlled by a pump. Different from the traditional valve-controlled hydraulic systems, the pump-controlled systems have higher energy efficiency. It is noted that the hydraulic systems play an important role in industry. But the systems are generally subject to nonlinearities, uncertainties, load disturbances (disturbance of the control signal), and measurement noises. Therefore, in precision position control cases, the challenge is how to compensate for these issues and obtain good tracking performance.

The last two decades have witnessed the increasing attention to the sliding mode control (SMC) which is inherently robust against the system uncertainty and the external disturbance and has a good transient response [1]. Therefore, SMC has been applied to many practical systems including electrical motors [2], power systems [3], suspension systems [4, 5], robot manipulators [6], and underwater vehicles [7, 8]. In recent years, with the wide application of digital controllers, the discrete-time sliding mode control (DT-SMC) has attracted more attention [9, 10]. Different from the continuous-time SMC [11, 12], it is challenging to drive the plant to the designed sliding mode surface due to the finite sampling rate [13] under the discrete-time framework. Thus, the study on the reaching law for the DT-SMC is of practical importance. The authors in [13] proposed a sufficient and necessary reaching law under which the closed-loop system would be driven toward the sliding mode surface and the switching function should be strictly decreasing. The quasi sliding mode and quasi sliding mode band were defined for single-input systems and multiple-input systems in [14] and [15], respectively. In addition, a linear reaching law can be seen in [16].

On another research frontier, the H_∞ control is robust against the disturbance and the external noise. Moreover,

it is insensitive to the noise statistics and less sensitive than their H_2 counterparts to uncertainties [17–19]. Therefore, the H_∞ control scheme has attracted interest in the feedback control [20–29] since it was first introduced in 1989 [30]. Recently, the H_∞ control and filtering approaches were adopted in various settings and applications, such as [31–33] and the reference therein. In this paper, we employ the H_∞ control strategy to design the sliding mode surface. Not only the H_∞ performance but also the pole placement is considered to have a balance on the tracking performance and the control input.

As mentioned, the sliding mode and H_∞ control are robust to the system uncertainties, load disturbances, and external measurement noises. Thus, it is interesting to apply the combined sliding mode and H_∞ control for the precision position of the EHA system. Therefore, in this paper, we use the norm-bounded uncertainty to represent the nonlinearity induced by the friction. The load disturbance and the noise are both considered in the system modeling. An integral sliding mode surface under the discrete-time framework is introduced. In an ideal sliding mode motion, the switching function will keep zero under which we obtain the equivalent control law. However, the uncertainty, load disturbance, and noise are all involved in the ideal control law. To compensate for these terms, an observer is employed and a practical control law is proposed. The control law would drive the EHA system arbitrarily close to the design sliding mode surface with a quasi sliding mode band. The contribution of the paper can be summarized as follows: (1) In the system modeling, we not only consider the nonlinear friction and the measurement noise but also the load disturbance. The studied model is more generalized and practical. (2) An integral discrete-time sliding mode control strategy is proposed. In the proposed integral discrete-time sliding mode control, the sign function of the sliding manifold is avoided such that the chatting phenomenon is eliminated. (3) In order to consider the transient response and the control action indirectly, we employ the pole placement technique in the controller design.

The paper is organized as follows: Section 2 is focused on the system modeling and description; Section 3 provides the robust sliding mode tracking controller design including the sliding surface design, the stability and the H_∞ performance analysis, and the robust tracking controller design; simulation and comparison results are provided in Section 4; and Section 5 concludes this paper.

Notation The notations used in this paper are fairly standard. Superscript "T" and "−1" indicate matrix transposition and inverse, respectively; $l_2[0,\infty)$ is the space of square-norm infinite vectors, and for $\omega \in l_2[0,\infty)$, and the 2-norm is given by $\|\omega\|_2 = \sqrt{\sum_{k=0}^{\infty} \|\omega_k\|^2}$. In addition, in symmetric block matrices or long matrix expressions, we use * as an ellipsis for the terms that are introduced by symmetry. Matrices, if their dimensions are not explicitly stated, are assumed to be compatible for algebraic operations.

2 System modeling and preliminary

In this paper, we consider a particular EHA system, as shown in Fig. 1.

The main components of the EHA system include an electrical motor, pressure and position sensors, a bidirectional gear pump, a symmetrical actuator, and an accumulator sub-circuit [34]. The bidirectional fixed displacement gear pump supplies oil to drive the actuator. The symmetrical actuator (inflow equals with outflow) is connected with an external load. The motion of the load can be regulated by controlling the speed of the electrical motor.

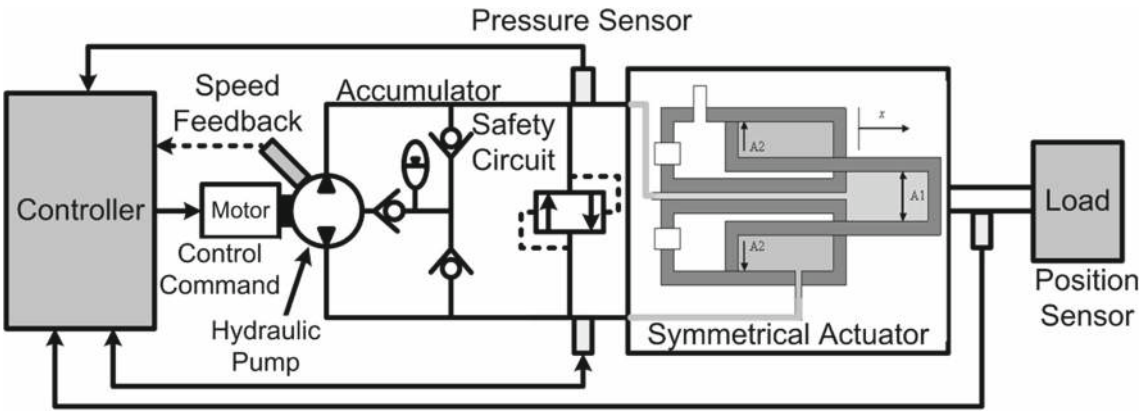

Fig. 1 Schematic of the EHA hydraulic circuit

To appropriately model the system, a discrete-time model with uncertainty, load disturbance, and measurement noises [35–37] is expressed as

$$X_{k+1} = (A + \Delta A)X_k + B[u_k + \Delta f(X_k, k)] + T_s w_k, \quad (1)$$

where $X_k=[x_{1k}, x_{2k}, x_{3k}]^T$; x_{1k}, x_{2k}; and x_{3k} represent the position, velocity, and acceleration of the load, respectively; u_k is the control input; $\Delta f(X_k,k)$ denotes the load disturbance; $T_s=0.001[1,1,1]^T$ and 0.001 is the sampling period; w_k is the measurement noise. In addition, the system matrix A and the input matrix B are identified as

$$A = \begin{bmatrix} 1 & 0.001 & 0 \\ 0 & 1 & 0.001 \\ 0 & -78.10 & 1.07 \end{bmatrix}, \; B = \begin{bmatrix} 0 \\ 0 \\ 1.07 \end{bmatrix}. \quad (2)$$

The system matrix is subject to uncertainty which comes from the nonlinearity of the friction. The uncertainty is described by the norm-bounded model as [37]

$$\Delta A = MD_kH = \begin{bmatrix} 0 \\ 0 \\ 0.1 \end{bmatrix} D_k [0 \quad 0.111 \quad 0.073], \quad (3)$$

with $-1 \le D_k \le 1$.

It is noted that the eigenvalues of the system matrix A are $\{1,\ 1.0350+0.2773i,\ 1.0350-0.2773i\}$ which are not within the unit circle, but the system is controllable. Moreover, the uncertainty ΔA affects the pole placement, that is, the uncertainty ΔA has an impact on the stability of the system. In addition, there are a load disturbance $\Delta f(X_k,k)$ at the controller side and a noise w_k which is either from the measurement noise or the quantization error. It is well known that the SMC has a good performance on the uncertainty and the H_∞ control is robust against the disturbance and the external noise. Therefore, in the following sections, the main objectives are to design the robust H_∞ sliding mode controller to stabilize the system (1) and apply the obtained results to the tracking control for the EHA system.

Remark 1 The system model in (1) is a generalized and practical model for the position control EHA systems. The system norm-bounded uncertain term ΔA is induced by the nonlinear friction. As the maximal and minimal nonlinear friction can be calibrated using experiments, the parameters in the norm-bounded uncertainties can be determined. The load disturbance can represent the quantization error of the control signal and the actuator faults. In addition, the noise term is necessary to denote the model errors which are assumed to be bounded.

3 Robust sliding mode tracking controller design for an EHA model

3.1 Robust sliding mode surface design and sliding mode dynamics analysis

Note that the uncertainty appears in the system matrix. In order to deal with the uncertainty, we introduce the following lemma.

Lemma 1 [38] Let $\Theta=\Theta^T$, $\overline{M}$, and $\overline{H}$ be real matrices with compatible dimensions, and D_k be time-varying and satisfy $-1 \le D_k \le 1$, then the following condition

$$\Theta + \overline{M}D_k\overline{H} + \overline{H}^T D_k \overline{M}^T < 0, \quad (4)$$

holds if and only if there exists a positive scalar $\varepsilon>0$ such that

$$\begin{bmatrix} \Theta & \varepsilon\overline{M} & \overline{H}^T \\ & -\varepsilon I & 0 \\ & * & -\varepsilon I \end{bmatrix} < 0 \quad (5)$$

is satisfied.

For the uncertain system (1), the integral sliding mode surface is constructed as

$$S(k) = GX_k - G\sum_{i=0}^{k-1}(A + BF - I)X_i, \quad (6)$$

where G is a matrix to be chosen such that GB is nonsingular and F is a feedback gain to be designed such that the system is stable. Note that the input matrix B has the dimension 3×1. In order to simplify the design, the matrix G can be chosen as the left inverse of B, that is, $GB=I$.

For an ideal sliding mode, the sliding surface $S(k)$ should converge to zero as the time k increases, that is,

$$S(k+1) = S(k) = 0, \ \text{for } k > k^*, \quad (7)$$

where k^* is a positive constant. When the trajectories of the EHA system enter into the sliding mode surface (6), we can obtain the equivalent control signal

$$\overline{u}_k = FX_k - G\Delta AX_k - \Delta f(X_k, k) - GT_s w_k. \quad (8)$$

By substituting the equivalent control signal into the EHA system (1), we derive the sliding mode dynamics on the sliding mode surface $S(k)=0$ as

$$X_{k+1} = (\overline{A} + M\underline{M}D_kH)X_k + \overline{B}w_k, \quad (9)$$

where

$$\overline{A} = A + BF, M\underline{M} = (I - BG)M, \overline{B} = (T_s - BGT_s).$$

Note that the location of the eigenvalues of the system (9) has a significant impact on the transient response. In order to trade off between the performance and the control input, we impose a circular regional constraint [39] on the pole location of the system (9). As shown in Fig. 2, it is required that the eigenvalues of the system (9) lie in the circle with the center point $(\sigma,0)$ and the nonzero radius r.

To evaluate the influence of the noise w_k, we assume that it is l_2-bounded and introduce the H_∞ performance of the transfer function from w_k to z_k,

$$z_k = X_k. \tag{10}$$

In summary, we focus on studying the H_∞ performance of the following system:

$$\begin{aligned} X_{k+1} &= (\bar{A} + \underline{M} D_k H) X_k + \bar{B} w_k, \\ z_k &= X_k. \end{aligned} \tag{11}$$

Lemma 2 [40] Suppose that the matrix F is known. For a positive scalar γ, the system (12) is asymptotically stable with an H_∞ performance γ if and only if there exists a matrix $P=P^{\mathrm{T}}>0$ such that the following condition is satisfied:

$$\begin{bmatrix} -P & 0 & P\left(\bar{A} + \underline{M} D_k H\right) & P\bar{B} \\ & -I & I & 0 \\ & * & -P & 0 \\ & * & * & -\gamma^2 I \end{bmatrix} < 0. \tag{12}$$

It is necessary to emphasize that there is one time-varying parameter D_k in the above condition. Moreover, the requirement of the pole location has not been considered in Lemma 1. Based on the result in Lemma 1, we develop the following theorem which eliminates the time-varying parameter and consider the pole location.

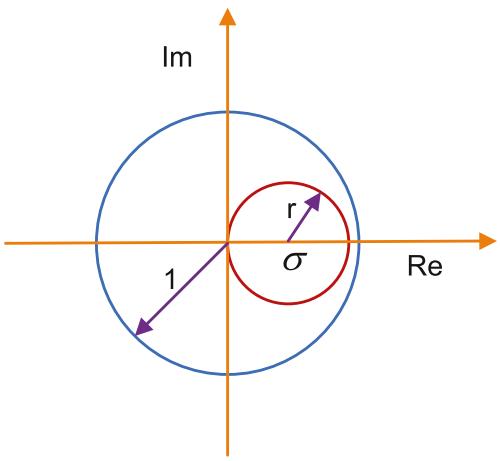

Fig. 2 Circular region (σ,r) for the pole location

Theorem 1 For a positive scalar γ, the system (11) is robustly asymptotically stable with an H_∞ performance γ and eigenvalues are all within the circular region (σ,r) if and only if there exist a matrix $Q=Q^{\mathrm{T}}>0$, a positive scalar ε, and a matrix $\overline{F}$ such that the following condition is satisfied:

$$\begin{bmatrix} -Q & 0 & \left(AQ + B\overline{F} - \sigma I\right)/r & \bar{B} & \varepsilon M/r & 0 \\ & -I & Q & 0 & 0 & 0 \\ & * & -Q & 0 & 0 & QH^{\mathrm{T}} \\ & * & * & -\gamma 2I & 0 & 0 \\ & * & * & * & -\varepsilon I & 0 \\ & * & * & * & * & -\varepsilon I \end{bmatrix} < 0. \tag{13}$$

Moreover, the feedback gain F can be calculated by $F = \overline{F} Q^{-1}$.

Proof: The condition in Lemma 2 can be rewritten as

$$\Theta + \overline{M} D_k \overline{H} + \overline{H}^{\mathrm{T}} D_k \overline{M}^{\mathrm{T}} < 0, \tag{14}$$

where

$$\Theta = \begin{bmatrix} -P & 0 & P\bar{A} & P\bar{B} \\ & -I & I & 0 \\ & * & -P & 0 \\ & * & * & -\gamma 2I \end{bmatrix},$$

$$\overline{M} = \begin{bmatrix} P\underline{M} \\ 0 \\ 0 \\ 0 \end{bmatrix}, \quad \overline{H} = [0 \quad 0 \quad H \quad 0].$$

According to Lemma 1, the condition (14) holds if and only if the following condition is satisfied:

$$\begin{bmatrix} -P & 0 & P\bar{A} & P\bar{B} & \varepsilon P\underline{M} & 0 \\ & -I & I & 0 & 0 & 0 \\ & * & -P & 0 & 0 & H^{\mathrm{T}} \\ & * & * & -\gamma^2 I & 0 & 0 \\ & * & * & * & -\varepsilon I & 0 \\ & * & * & * & * & -\varepsilon I \end{bmatrix} < 0. \tag{15}$$

Performing a congruence transformation to (15) by $J=\mathrm{diag}\{Q,I,Q,I,I,I\}$, we get

$$\begin{bmatrix} -Q & 0 & AQ + BFQ & \bar{B} & \varepsilon\underline{M} & 0 \\ & -I & Q & 0 & 0 & 0 \\ & * & -Q & 0 & 0 & QH^{\mathrm{T}} \\ & * & * & -\gamma^2 I & 0 & 0 \\ & * & * & * & -\varepsilon I & 0 \\ & * & * & * & * & -\varepsilon I \end{bmatrix} < 0, \tag{16}$$

where $Q=P^{-1}$. Letting $\overline{F}$ denote the multiplication FQ, (16) is equivalent with

$$\begin{bmatrix} -Q & 0 & AQ+BF & \bar{B} & \varepsilon \underline{M} & 0 \\ & -I & Q & 0 & 0 & 0 \\ & * & -Q & 0 & 0 & QH^{\mathrm{T}} \\ & * & * & -\gamma^2 I & 0 & 0 \\ & * & * & * & -\varepsilon I & 0 \\ & * & * & * & * & -\varepsilon I \end{bmatrix} < 0. \quad (17)$$

By using $(A+\underline{M}D_kH-\sigma I)/r$ to replace $(A+\underline{M}D_kH)$ in Lemma 2 and following similar lines from (14) to (17), we can obtain the condition (13). On the other hand, since Q is nonsingular, F can be computed with $F=\overline{F}Q^{-1}$.

Theorem 1 provides the design method for the feedback gain F with a fixed H_∞ performance γ. In practice, it is required that the value for γ is as smaller as possible. The following corollary addresses the optimization method for the minimal value.

Corollary 1 The minimum H_∞ performance index γ^* in Theorem 1 can be found by solving the following convex optimization problem:

$$\beta = \min \gamma^2 \cdot \quad s.t.(13)$$

The corresponding minimum value for γ is $\gamma^{\frown} = \sqrt{\beta}$.

3.2 Robust sliding mode controller design

In the above subsection, we have proposed the sliding mode surface, analyzed the H_∞ performance of the sliding mode dynamics, and obtained the equivalent control signal. However, since both the load disturbance and the noise are involved in the equivalent control signal, we cannot directly apply the equivalent control signal $\overline{u}$ to the control signal u_k. In this subsection, we explore the control law and reaching condition.

In this paper, we adopt the linear reaching law [16]:

$$S(k+1) = \Phi S(k), \quad (18)$$

where Φ is a scalar and $0 \le \Phi < 1$. It is worth mentioning that the reaching law (18) implies $|S(k+1)|<|S(k)|$ which is a necessary and sufficient condition to assure the convergence of a discrete-time sliding mode control system in [13]. Due to the lack of knowledge of the disturbance and noise, the ideal sliding mode control law cannot be implemented. However, we can predict the disturbance and noise with the value at the previous time [41, 42]. At the time k, we can obtain the lumped uncertainty, disturbance, and noise at the time $k-1$. Suppose that

$$g_{k-1} = X_k - AX_{k-1} - Bu_{k-1}. \quad (19)$$

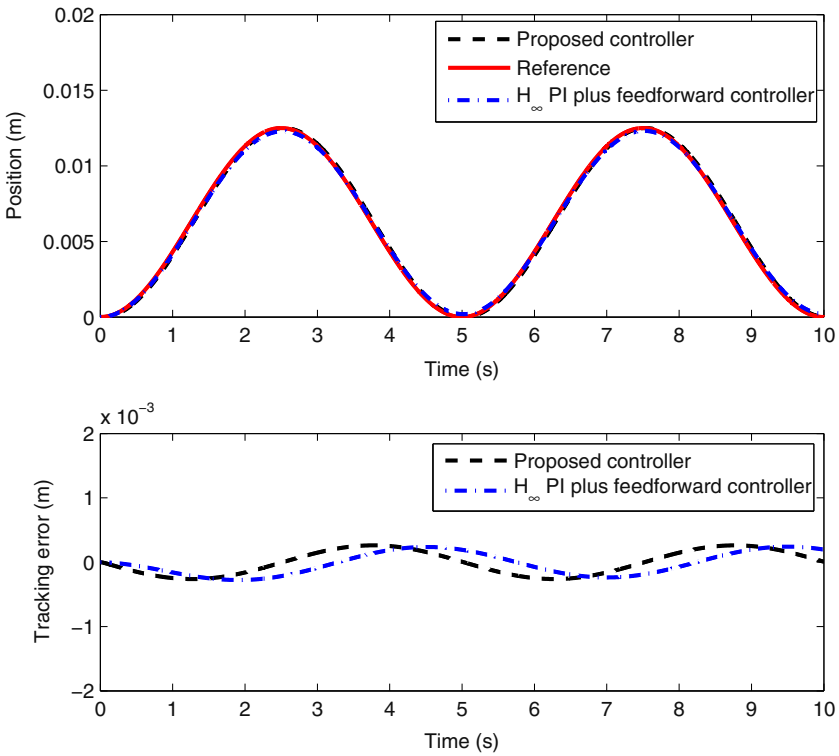

Fig. 3 Control performance comparison with the optimal H_∞ PI plus feedforward controller

Then, the proposed control law in this paper is expressed as

$$u_k = FX_k - Gg_{k-1} + (\Phi - 1)S(k), \tag{20}$$

where F is the gain designed in the above subsection. Now, we will prove that the reaching law in (18) can be satisfied under the control law (20).

Theorem 2 For the uncertain EHA system, suppose that there is a feasible solution for the feedback gain F in Theorem 1, then under the control law (20), the EHA system will be driven arbitrarily close to the quasi sliding mode surface and the corresponding band Δ is

$$\Delta = \frac{\widehat{g}}{1-\Phi}, \tag{21}$$

where $\widehat{g}$ is the maximal value of $|G(g_k - g_{k-1})|$.

Proof: By substituting the control law (20) into the system model (1), we evaluate the difference of $S(k)$ as

$$S(k+1) - S(k) = Gg_k - Gg_{k-1} + (\Phi - 1)S(k), \tag{22}$$

which implies that

$$S(k+1) = G(g_k - g_{k-1}) + \Phi S(k). \tag{23}$$

Suppose that the initial value for the sliding mode surface is $S(0)$. According to (23), the value for $S(k)$ is

$$S(k) = \sum_{i=1}^{k-1} \Phi^i G(g_i - g_{i-1}) + \Phi^k S(0). \tag{24}$$

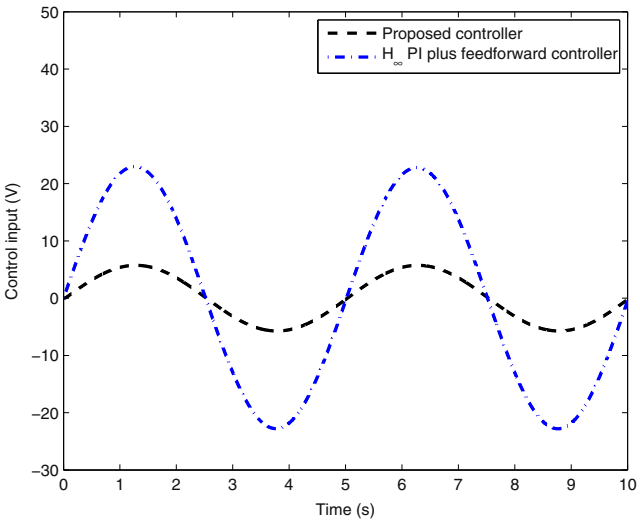

Fig. 4 Control input comparison with the optimal H_∞ PI plus feedforward controller

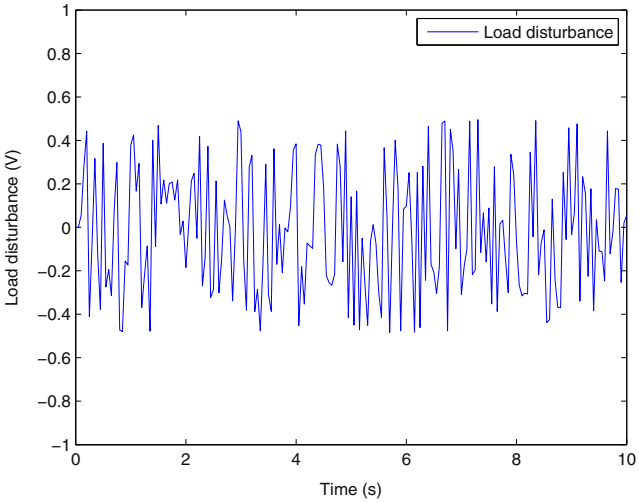

Fig. 5 The disturbance at the controller

It is noted that $|\Phi|<1$. Thus, for a large k, $\Phi^k S(0)$ will converge to zero and

$$|S(k)| < \frac{\widehat{g}}{1-\Phi}. \tag{25}$$

The proof is completed.

Remark 2 It can be seen from the control law in (20) that the control signal consists of three terms: a state-feedback action, an observation feedback term, and a sliding mode manifold feedback term. Generally speaking, the state-feedback action has the capacity to stabilize the system or relocate the eigenvalue location of the closed-loop system matrix. The observation sliding mode manifold feedback is used to compensate for the system uncertainty, the load disturbance, and the external term. Moreover, it is necessary to mention that the system dynamics is involved in the sliding mode surface and the sign function of the sliding mode surface is avoided in the

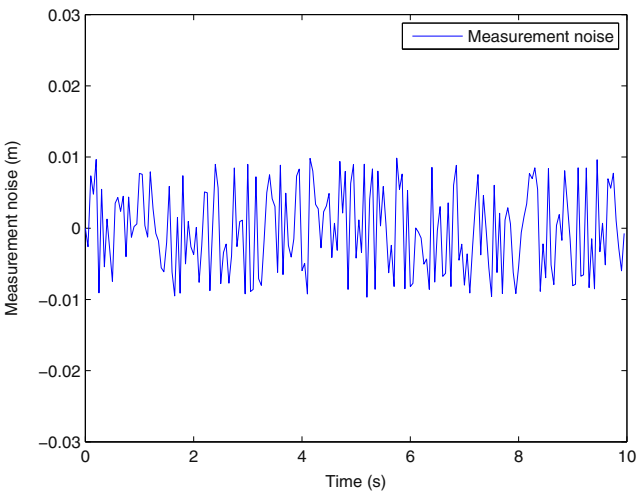

Fig. 6 Measurement noise for the EHA system

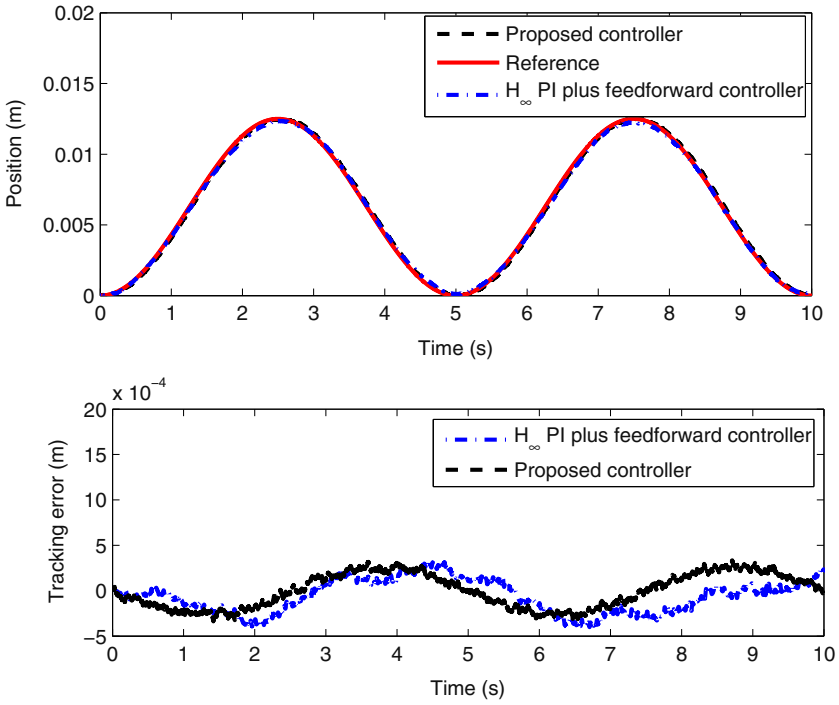

Fig. 7 Control performance comparison with the optimal H_∞ PI plus feedforward controller

control law in (20). Thus, the chatting phenomenon of the traditional SMC can be eliminated.

3.3 Robust sliding mode tracking control

In the above two subsections, we have investigated the stabilization problem for the discrete-time EHA system subject to uncertainty, load disturbance, and noise. In the state tracking problem, we assume that the desired states X_{dk} of the EHA system satisfy the nonlinear model. Defining the tracking error as $X_{ek}=X_k-X_{dk}$, the sliding mode surface for the tracking error system is

$$S_e(k) = GX_{ek} - G\sum_{i=0}^{k-1}(A+BF-I)X_{ei}, \tag{26}$$

and the control law is

$$u_k = FX_{ek} - G\overline{g}_{k-1} + (\Phi - 1)S_e(k), \tag{27}$$

where

$$\overline{g}_{k-1} = X_{ek} - AX_{e(k-1)} - Bu_k, \tag{28}$$

and F can be calculated in Corollary 1.

4 Simulation results

In this section, we apply the developed discrete-time sliding mode tracking control to the EHA system which is subject to nonlinearity, load disturbance, and noise. Suppose that the desired circular region (σ,r) is (0.9,0.05). By using Corollary 1, the obtained minimum H_∞ performance index is 300.6335 and the corresponding feedback gain $F = [-7007.3 \quad 49.63 \quad -0.32]$.

The authors of Chapter 12 in [43] designed an H_∞ proportional-integral (PI) plus feedforward controller for the same EHA system. The control law is a PI feedback control plus a feedforward term as follows:

$$u_k = K_p e_k + K_i \sum_{i=0}^{k-1} e_i + K_{ff}(r_k - r_{k-1}), \tag{29}$$

where K_p=2,428.6, K_i=20.2, K_{ff}=2,860,000, r_k is the desired position trajectory, and e_k is the tracking error. In order to do a fair comparison in the simulation studies, we assume that there is no load disturbance in the control action and noise in the measurements. Figure 3 shows the tracking control performance comparison between the proposed discrete-time integral sliding mode controller and the optimal H_∞ PI plus feedforward controller. We can see that, for the sinusoid signal, both controllers can track the reference well and the tracking errors are at the same level. However, it infers from Fig. 4 that the control

Table 1 Tracking error comparison

Controller	2 norm	Infinity norm
Proposed controller	0.0188	3.5889×10^{-4}
H_∞ PI plus feedforward controller	0.0192	4.0955×10^{-4}

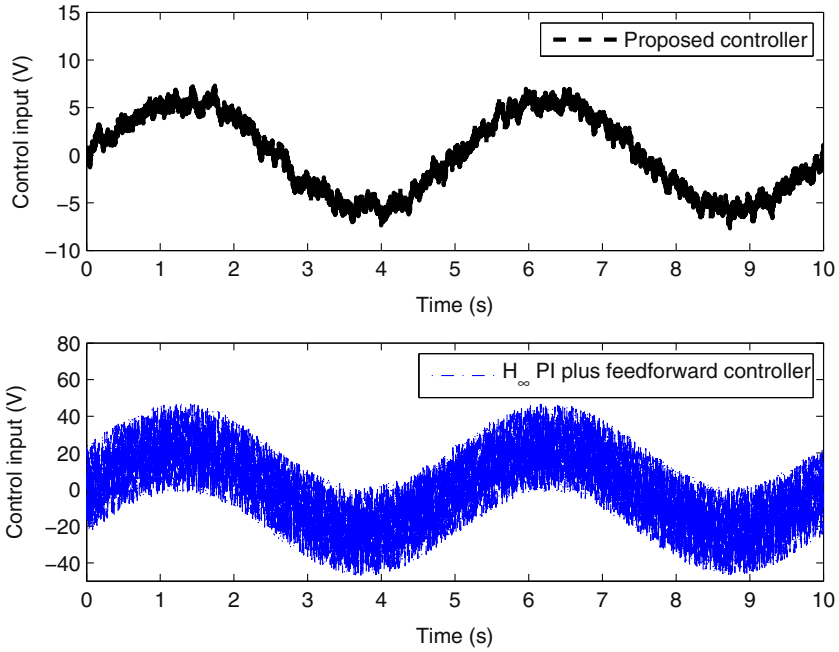

Fig. 8 Control input comparison with the optimal H_∞ PI plus feedforward controller

input is the optimal H_∞ PI plus feedforward controller is around 5 times of the proposed controller in this paper, that is, the optimal H_∞ PI plus feedforward controller would consume much more energy for a similar control performance. Considering the tracking performance and the consumed energy simultaneously, the proposed tracking controller in this paper is much better than the one in [43].

The system uncertainty, load disturbance, and measurement noise are all incorporated in the controller design. Moreover, the lumped disturbance predictor is used to compensate for all the uncertainty and load

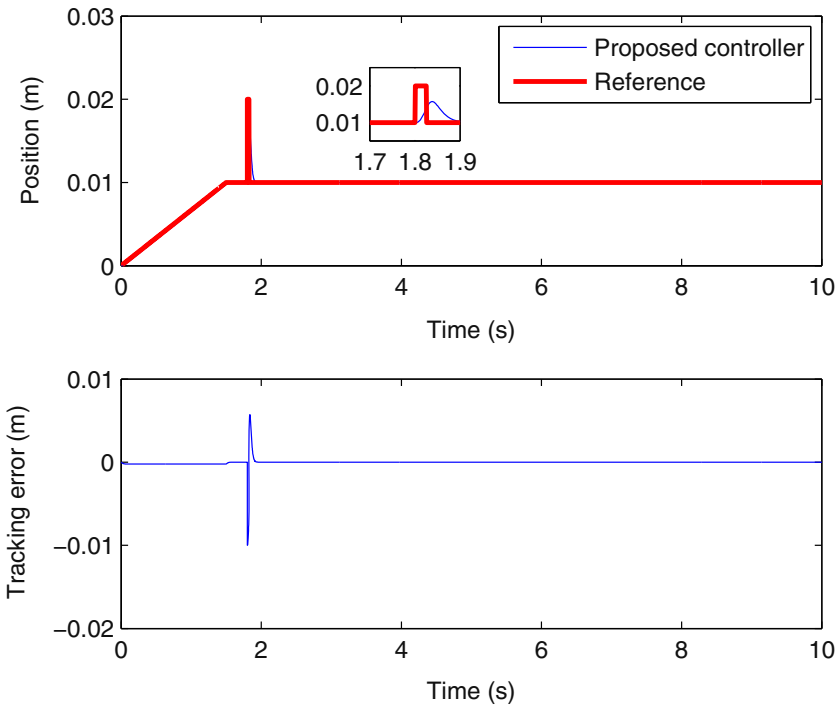

Fig. 9 Tracking control performance of an abrupt reference

disturbance. To show the advantage of the proposed controller, in the simulation, the added load disturbance at the control signal and the noise are illustrated in Figs. 5 and 6, respectively. By choosing Φ as 0.1, Fig. 7 shows the tracking performance comparison when the desired position is a sinusoid wave. The tracking error comparison is illustrated in Table 1.

As shown in Table 1, both the 2 norm and the infinity norm of the tracking error with the proposed controller are smaller than the corresponding one of the H_∞ PI plus feedforward controller.

Figure 8 depicts the control input comparison. When the system is subject to the uncertainty, load disturbance, and the measurement noise, the control input of the optimal H_∞ PI plus feedforward controller fluctuates significantly, that is, the control input of the optimal H_∞ PI plus feedforward controller is sensitive to the noises. However, the designed control has the capacity to maintain the control performance with much smaller and smoother control signal.

To show the tracking performance of the proposed controller when there is an abrupt change at the reference, a quasi step signal is acted as the reference. The reference is subject to an abrupt change at 1.8 s, and the change lasts for 0.025 s. Figure 9 depicts the tracking control performance of the proposed controller. It can be seen that the undesired response is much smaller than the abrupt change, that is, the proposed controller has a good performance at attenuating the effect of abrupt change.

5 Conclusions

In this paper, we have investigated the sliding mode control for the EHA system. The nonlinear EHA system was modeled by a linear system with norm-bounded uncertainty. The load disturbance and the measurement noise were both considered in the modeling. An integral sliding mode surface was proposed. After obtaining the equivalent control signal, the design approach for the feedback gain was addressed. By using a well-known reaching condition, a sliding mode control law was developed such that the EHA system can be driven to the quasi sliding mode surface. In the system modeling, the nonlinear friction was represented by the norm-bounded uncertainty. The designed controller has the stability margin such that it is robust to the norm-bounded uncertainty. Generally speaking, the designed controller is passive uncertainty tolerable. In the future research, we will employ the Takagi-Sugeno (T-S) [44–48] fuzzy model and the backstepping technique [49, 50] to study the system.

Acknowledgments The authors wish to thank the associate editor and the anonymous reviewers for providing constructive suggestions which have improved the presentation of the paper.

References

1. Utkin V, Guldner J, Shi J (1999) Sliding mode control in electromechanical systems. CRC Press, Boca Raton
2. Utkin VI (1993) Sliding mode control design principles and applications to electric drives. IEEE Trans Ind Electron 40(1): 23–36
3. Vidal-Idiarte JCE, Martinez-Salamero L, Romero A (2006) An H_∞ control strategy for switching converters in sliding-mode current control. IEEE Trans Power Electron 21(2):553–556
4. Huang S-J, Chen H-Y (2006) Adaptive sliding controller with self-tuning fuzzy compensation for vehicle suspension control. Mechatronics 16(10):607–622
5. Sam YM, Osman JHS, Ghani MRA (2004) A class of proportional-integral sliding mode control with application to active suspension system. Syst Contr Lett 51(3–4):217–223
6. Parra-Vega V, Hirzinger G (2001) Chattering-free sliding mode control for a class of nonlinear mechanical systems. Int J Robust Nonlinear Control 11(12):1161–1178
7. Wu L, Shi P, Gao H (2010) State estimation and sliding-mode control of Markovian jump singular systems. IEEE Trans Autom Contr 55(5):1213–1219
8. Wu L, Ho DWC (2010) Sliding mode control of singular stochastic hybrid systems. Automatica 46(4):779–783
9. Chang J-L (2008) Robust discrete-time model reference sliding-mode controller design with state and disturbance estimation. IEEE Trans Ind Electron 55(11):4065–4074
10. Lai NO, Edwards C, Spurgeon SK (2007) On output tracking using dynamic output feedback discrete-time sliding-mode controllers. IEEE Trans Autom Contr 52(10):1975–1981
11. Choi HH (1999) On the existence of linear sliding surfaces for a class of uncertain dynamic systems with mismatched uncertainties. Automatica 35(10):1707–1715
12. Wu L, Zheng WX (2009) Passivity-based sliding mode control of uncertain singular time-delay systems. Automatica 45(9):2120–2127
13. Sarpturk SZ, Istefanopulos Y, Kaynak O (1987) On the stability of discrete-time sliding mode control systems. IEEE Trans Autom Contr 32(10):930–932
14. Gao W, Wang Y, Homaifa A (1995) Discrete-time variable structure control systems. IEEE Trans Ind Electron 42(2):117–122
15. Bartoszewicz A (1996) Remarks on discrete-time variable structure control systems. IEEE Trans Ind Electron 43(1):235–238
16. Hui S, Żak SH (1999) On discrete-time variable structure sliding mode control. Syst Contr Lett 38(4–5):283–288
17. Fridman E, Shaked U, Xie L (2003) Robust H_∞ filtering of linear systems with time-varying delay. IEEE Trans Autom Contr 48(1): 159–165
18. Zhang H, Shi Y, Saadat Mehr A (2011) Robust weighted H_∞ filtering for networked systems with intermitted measurements of multiple sensors. Int J Adapt Control Signal Process 25(4):313–330
19. Zhang H, Zhang X, Wang J (2014) Robust gain-scheduling energy-to-peak control of vehicle lateral dynamics stabilisation. Vehicle Syst Dyn 52(3):309–340
20. Walker KC, Pan Y-J, Gu J (2009) Bilateral teleoperation over networks based on stochastic switching approach. IEEE/ASME Trans Mechatronics 14(5):539–554
21. Hua C-C, Liu XP (2013) A new coordinated slave torque feedback control algorithm for network-based teleoperation systems. IEEE/ASME Trans Mechatronics 18(2):764–774

22. Xu P, Peticca G, Wong D (2008) A technique for developing a high accuracy durability test for a light truck on a six degree-of-freedom road test simulator. Int J Vehicle Design 47(1–4):290–304
23. Islam S, Liu PX (2011) Robust adaptive fuzzy output feedback control system for robot manipulators. IEEE/ASME Trans Mechatronics 16(2):288–296
24. Ye Y, Liu PX (2010) Improving trajectory tracking in wave-variable-based teleoperation. IEEE/ASME Trans Mechatronics 15(2):321–326
25. Islam S, Liu PX (2011) PD output feedback control design for industrial robotic manipulators. IEEE/ASME Trans Mechatronics 16(1):187–197
26. Xu P, Bernardo B, Tan K (2011) Optimal mounting design for cab vibration isolation. Int J Vehicle Design 57(2–3):292–304
27. Huang J, Shi Y, Wu J (2012) Transparent virtual coupler design for networked haptic systems with a mixed virtual wall. IEEE/ASME Trans Mechatronics 17(3):480–487
28. Zhang H, Shi Y, Saadat Mehr A (2012) Robust H_∞ PID control for multivariable networked control systems with disturbance/noise attenuation. Int J Robust Nonlinear Control 22(2):183–204
29. Lee C, Salapaka SM (2009) Fast robust nanopositioning—a linear-matrix-inequalities-based optimal control approach. IEEE/ASME Trans Mechatronics 14(4):414–422
30. Elsayed A, Grimble MJ (1989) A new approach to the H_∞ design of optimal digital linear filters. IMA J Math Control Inform 6(2):233–251
31. Fallah MS, Bhat RB, Xie WF (2012) Optimized control of semiactive suspension systems using H_∞ robust control theory and current signal estimation. IEEE/ASME Trans Mechatronics 17(4):767–778
32. Dong H, Wang Z, Gao H (2009) H_∞ fuzzy control for systems with repeated scalar nonlinearities and random packet losses. IEEE Trans Fuzzy Syst 17(2):440–450
33. Dong H, Wang Z, Ho DWC, Gao H (2010) Robust H_∞ fuzzy output-feedback control with multiple probabilistic delays and multiple missing measurements. IEEE Trans Fuzzy Syst 18(4):712–725
34. Habibi SR, Goldenberg AA (2000) Design of a new high-performance electrohydraulic actuator. IEEE/ASME Trans Mechatron 5(2):158–165
35. Habibi SR, Sigh G (2000) Derivation of design requirements of optimization of a high performance hydrostatic actuation system. Int J Fluid Power 2(1):11–27
36. Wang S, Habibi SR, Burton R, Sampson E (2008) Sliding mode control for an electrohydraulic actuator system with discontinuous non-linear friction. Proc Inst Mech Eng J Syst Control Eng 222(8):799–815
37. Lin Y, Shi Y, Burton R (2013) Modeling and robust discrete-time sliding-mode control design for a fluid power electrohydraulic actuator (EHA) system. IEEE/ASME Trans Mechatron 18(1):1–10
38. Wang Z, Yang F, Ho DWC, Liu X (2006) Robust H_∞ filtering for stochastic time-delay systems with missing measurements. IEEE Trans Signal Process 54(7):2579–2587
39. Haddad WM, Bernstein DS (1992) Controller design with regional pole constraints. IEEE Trans Autom Contr 37(1):54–69
40. Gao H, Lam J, Xie L, Wang C (2005) New approach to mixed H_2/H_∞ filtering for polytopic discrete-time systems. IEEE Trans Signal Process 53(8):3183–3192
41. Morgan R, Ozguner O (1985) A decentralized variable structure control algorithm for robotic manipulators. IEEE Trans Autom Contr 1(1):57–65
42. Su W-C, Drakunov SV, Ozguner O (2000) An $O(T^2)$ boundary layer in sliding mode for sampled-data systems. IEEE Trans Autom Contr 45(3):482–485
43. Zhang D (ed) (2013) Advanced mechatronics and MEMS devices. Springer, London
44. Su X, Shi P, Wu L, Song Y-D (2012) A novel approach to filter design for t-s fuzzy discrete-time systems with time-varying delay. IEEE Trans Fuzzy Syst 20(6):1114–1129
45. Zhang H, Shi Y, Liu MX (2013) H_∞ step tracking control for networked discrete-time nonlinear systems with integral and predictive actions. IEEE Trans Ind Informat 9(1):337–345
46. Su X, Wu L, Shi P, Song Y-D (2012) H_∞ model reduction of T-S fuzzy stochastic systems. IEEE Trans Syst Man Cybern B 42(6):1574–1585
47. Zhang H, Shi Y, Saadat Mehr A (2012) On H_∞ filtering for discrete-time Takagi-Sugeno fuzzy systems. IEEE Trans Fuzzy Syst 20(2):396–401
48. Zhang H, Shi Y, Wang J (2014) On energy-to-peak filtering for nonuniformly sampled nonlinear systems: a Markovian jump system approach. IEEE Trans Fuzzy Syst 22(1):212–222
49. Wei L, Fang F, Shi Y (2013) Adaptive backstepping-based composite nonlinear feedback water level control for the nuclear u-tube steam generator. IEEE Trans Contr Syst Technol. doi:10.1109/TCST.2013.2250504
50. Fang F, Wei L (2011) Backstepping-based nonlinear adaptive control for coal-fired utility boiler-turbine units. Appl Energ 88(3):814–824